

Copyright © 1994, by the author(s).  
All rights reserved.

Permission to make digital or hard copies of all or part of this work for personal or classroom use is granted without fee provided that copies are not made or distributed for profit or commercial advantage and that copies bear this notice and the full citation on the first page. To copy otherwise, to republish, to post on servers or to redistribute to lists, requires prior specific permission.

**SIDEWALL FORCING OF HEXAGONAL TURING  
PATTERNS: RHOMBIC PATTERNS**

by

V. Pérez-Muñuzuri, M. Gómez-Gesteira, A. P. Muñuzuri,  
L. O. Chua, and V. Pérez-Villar

Memorandum No. UCB/ERL M94/35

1 April 1994

COVER PAGE

---

**This work is supported in part by the Office of Naval Research under grant N00014-93-1-1361 and the National Science Foundation under grant MIP-9114168.**

**SIDEWALL FORCING OF HEXAGONAL TURING  
PATTERNS: RHOMBIC PATTERNS**

by

V. Pérez-Muñuzuri, M. Gómez-Gesteira, A. P. Muñuzuri,  
L. O. Chua, and V. Pérez-Villar

Memorandum No. UCB/ERL M94/35

1 April 1994

**ELECTRONICS RESEARCH LABORATORY**

College of Engineering  
University of California, Berkeley  
94720

**SIDEWALL FORCING OF HEXAGONAL TURING  
PATTERNS: RHOMBIC PATTERNS**

by

V. Pérez-Muñuzuri, M. Gómez-Gesteira, A. P. Muñuzuri,  
L. O. Chua, and V. Pérez-Villar

Memorandum No. UCB/ERL M94/35

1 April 1994

**ELECTRONICS RESEARCH LABORATORY**

College of Engineering  
University of California, Berkeley  
94720

---

**This work is supported in part by the Office of Naval Research under grant N00014-93-1-1361 and the National Science Foundation under grant MIP-9114168.**

# SIDEWALL FORCING OF HEXAGONAL TURING PATTERNS: RHOMBIC PATTERNS

V. Pérez-Muñuzuri, M. Gómez-Gesteira, A.P. Muñuzuri, L.O. Chua<sup>1</sup>

and V. Pérez-Villar

*Group of Nonlinear Physics  
Faculty of Physics  
University of Santiago de Compostela  
15706 Santiago de Compostela, Spain.*

*E-Mail: uscfmvpm@cesga.es*

April 1994

## Abstract

Rhombic arrays were obtained by sidewall forcing during Turing pattern formation. Locking between the frequency of forcing and the wave length between blobs in accordance with the Farey sequence was obtained. This locking being represented by a perfect rhombic array oriented in the direction of the imposed forcing. For a constant forcing in duration and amplitude, the following scheme of bifurcation was observed: parallel stripes  $\mapsto$  rhombic array  $\mapsto$  domains of hexagons and rhombi separated by "penta-hepta" defects. Symmetry considerations based on a non-uniform stretching along the x-axis was used to describe these transitions. Unstable "varicose-vein" stripes were observed to evolve during the temporal evolution of rhombic arrays.

---

<sup>1</sup>Permanent address: Dept. of Electrical Engineering and Computer Sciences. Univ. of California at Berkeley, CA 94720, USA.

## 1. Introduction

The effect of imposed spatial or temporal modulations on pattern-forming systems has been analyzed recently in various experimental and theoretical situations [1,2]. For example, periodic spatial forcing imposed on a system which undergoes a pattern-forming instability may induce transitions between structures with incommensurate wavelengths [3,4] or lead to continuous variations of the wavelength of the pattern [5]. On the other hand, purely temporal modulations of the bifurcation parameter have also been studied [6,7], as in the case of Rayleigh-Bénard instabilities where a temporal modulation of the temperature gradient may trigger the formation of hexagonal planforms [8,9]. Temporal modulation of an external field applied on the Belousov-Zhabotinsky reaction is able to disorganize spiral waves leading to spatial disorder [10] or to induce the drift of the spiral waves [11-14]. Thus, in two-dimensional systems, pattern selection and stability [9,15] may be strongly affected by externally imposed modulations as discussed by Pismen [16].

Hexagonal patterns constitute an important subject of research in the theory of Turing and convection structures. They are easily observed in Rayleigh-Bénard convection, in non-Boussinesq fluids [17,18], in Bénard-Marangoni convection [19-21], within starch-gels in reaction-diffusion systems [22-24], etc. However, perfect hexagonal patterns are rather difficult to observe in large-aspect ratio systems. Typically, different line or point defects appear in the background of a hexagonal pattern. Among point defects, the most typical are the so called "penta-hepta" defects, or pair of cells with five and seven ridges. These defects, once having been created, are very stable [18] and separate multiple domains of hexagons with different orientations [25-27].

On the other hand, although the effect of global spatial or temporal

modulation have been widely studied, little has been done on the effect of local forcing on Turing structures [28-30]. Periodic sidewall forcing on Turing patterns mimics the behavior of the boundary between two domains; one, where periodic wave trains propagate through the medium and the other, where Turing structures are developing.

The purpose of this paper is to study in numerical experiments the conditions under which defects disappear when sidewall forcing occurs in a reaction-diffusion systems undergoing a Turing bifurcation. This kind of forcing is shown to perfectly re-organize the systems in form of a rhombic array. The influence of the frequency of forcing in the bifurcation between the different patterns; stripes, rhombi and hexagons is presented in this paper.

## 2. Numerical Model and Theory

Turing structures can be numerically described by many systems of reaction-diffusion partial differential equations such that its homogeneous steady state can become unstable due to random disturbances. In particular, the ratio between diffusion coefficients plays an important role in Turing pattern formation. Since Turing's classical paper in 1952 [28], multitude of numerical models have been suggested in order to describe these structures. In this paper, we use a set of discretely-coupled dynamical systems, each cell/unit being described by a Chua's circuit [31], in order to describe the regular appearance of rhombi when sidewall forcing is applied into the medium. Our motivation for choosing this system is that arrays of Chua's circuits can be fabricated into a VLSI chip which allows real-time experiments where all the parameters can be controlled easily and with higher accuracy than in chemical media. The most important difference of this system from those studied previously is its discrete (in space) nature which gives rise to

slightly different set of conditions for Turing pattern formation.

The set of discretely-coupled system of ordinary differential equations is

$$\begin{aligned}
 \dot{u}_{i,j} &= \alpha \left\{ v_{i,j} - h(u_{i,j}) \right\} + D_u \left\{ u_{i+1,j} + u_{i-1,j} + u_{i,j+1} + u_{i,j-1} - 4u_{i,j} \right\} \\
 \dot{v}_{i,j} &= u_{i,j} - v_{i,j} + w_{i,j} + D_v \left\{ v_{i+1,j} + v_{i-1,j} + v_{i,j+1} + v_{i,j-1} - 4v_{i,j} \right\} \\
 \dot{w}_{i,j} &= -\beta v_{i,j} - \gamma w_{i,j} \quad (i,j = 1 \dots n)
 \end{aligned} \tag{1}$$

where  $h(u)$  describes a continuous three-segment piece-wise-linear curve of the nonlinear characteristic described by  $h(u) = m_1 u + 0.5(m_0 - m_1)(|u+1| - |u-1|) + \epsilon$  ( $\epsilon$  is a constant related to the excitability of the system [32]). Here  $m_0$  and  $m_1$  denote the slopes of the three segments.

In order to describe the limits of validity of our equations for Turing pattern formation we can reduce the set of equations (1) to,

$$\begin{aligned}
 \dot{u}_{i,j} &= \alpha \left\{ v_{i,j} - h(u_{i,j}) \right\} + D_u \left\{ u_{i+1,j} + u_{i-1,j} + u_{i,j+1} + u_{i,j-1} - 4u_{i,j} \right\} \\
 \dot{v}_{i,j} &= u_{i,j} - \nu v_{i,j} + D_v \left\{ v_{i+1,j} + v_{i-1,j} + v_{i,j+1} + v_{i,j-1} - 4v_{i,j} \right\}
 \end{aligned} \tag{2}$$

Since the parameters  $\alpha$ ,  $\beta$  and  $\gamma$  in our study are chosen such that  $w$  changes on the fastest time scale, we have assumed that  $w(\vec{r}, t)$  is always determined by the instantaneous values of  $u$  and  $v$  according to

$$w = -\frac{\beta}{\gamma} v$$

and  $\nu$  in equation (2) is a new parameter equal to  $(\gamma + \beta)/\beta$ . Here  $u$ ,  $v$  and  $w$  denote vectors whose components are  $u_{i,j}$ ,  $v_{i,j}$  and  $w_{i,j}$ , respectively. We also define  $\vec{r} = x\vec{i} + y\vec{j}$ .

Since we are concerned with Turing pattern formation or diffusion driven instability, we are interested in the linear (local) stability of the steady state of Eq.(2). Following Murray [29], we look for solutions in the form  $\exp\{i(kj-\lambda t)\}$  where  $k$  and  $\lambda$  are considered to be independent of the position<sup>2</sup>  $j$  ( $j = 1\dots n$ ), which differs from continuous dynamical systems where the coupling in Eq.(2) is represented by the Laplacian operator for the  $u$  and  $v$  variables and we seek for solutions of the form  $\exp\{i(k\vec{r}-\lambda t)\}$ .

Straightforward calculations give the following conditions for the generation of spatial patterns by a two-species reaction-diffusion mechanism of the form of Eq.(2)

$$\begin{aligned}
f_u + g_v &< 0 \\
f_u g_v - f_v g_u &> 0 \\
f_u D_v + g_v D_u &> 0 \\
\left\{f_u D_v + g_v D_u\right\}^2 - 4 D_u D_v \left\{f_u g_v - f_v g_u\right\} &> 0
\end{aligned} \tag{3}$$

where  $f_u$ ,  $f_v$ ,  $g_u$  and  $g_v$  are the partial derivatives of  $f$  and  $g$  (right side part of equations (2) without coupling) evaluated at the steady state. The critical wavenumber is given by

$$\cos(k_c) = 1 - \frac{f_u D_v + g_v D_u}{4 D_u D_v} \tag{4}$$

Equation (4) restricts the limit of Turing pattern formation such that

---

<sup>2</sup>For simplicity in the calculations, we consider here only the one-dimensional problem.

$$\left| \frac{f_u D_v + g_v D_u}{8 D_u D_v} \right| \leq 1 \quad (5)$$

The set of fixed parameters, satisfying conditions (3) to (5), used throughout this paper is  $\{\alpha, \nu, m_0, m_1, \epsilon\} = \{-10, 2, -1, 0.1, 2\}$ . Figure 1 shows the allowable values of  $D_u$  and  $D_v$  as a function of the critical wavenumber  $k_c$  satisfying equations (3) to (5). Note that for a given value of  $D_u$ ,  $k_c$  remains approximately constant for any  $D_v$ .

The periodic sidewall forcing to the system was modeled by periodically forcing the  $u$ -variable in Eq.(1) as follows

$$\begin{aligned} \dot{u}_{i,j} &= \alpha \left\{ v_{i,j} - h(u_{i,j}) \right\} + \\ &\quad D_u \left\{ u_{i+1,j} + u_{i-1,j} + u_{i,j+1} + u_{i,j-1} - 4u_{i,j} \right\} + A_p \cos(\omega t) \delta(i-1) \\ \dot{v}_{i,j} &= u_{i,j} - \nu v_{i,j} + D_v \left\{ v_{i+1,j} + v_{i-1,j} + v_{i,j+1} + v_{i,j-1} - 4v_{i,j} \right\} \end{aligned} \quad (6)$$

where  $A_p$  and  $\omega$  are the amplitude and frequency of forcing respectively and  $\delta(\cdot)$  is the Dirac's delta equal to one when  $i=1$  at any  $j \in [1, n]$  and zero otherwise.  $A_p$  was kept constant and set equal to one for all calculations shown in this paper.

The nonlinear boundary value problem described by Eqs.(6) was completed by imposing zero-flux boundary conditions. A uniform time step of 0.001 was used throughout as the differential equations were integrated using an explicit Euler method. Even though most of our simulations were carried out on a 50 x 50 grid, the effect of the grid size on Turing pattern formation was studied on grids as small as 30 x 30 and as large as 100 x 100. A random initial condition was chosen for all the variables in Eqs.(6) so that the average values were equal to their respective homogeneous fixed point values. Without forcing ( $A_p = 0$ ) the system evolves naturally from this random initial state to an hexagonal array with multiple defects.

hepta" defects and perfectly organized rhombic arrays within the resonant peaks. Parallel stripes were not observed.

For values of the frequency of forcing within the resonant peaks, rhombic arrays develop in time from an unstable striped pattern. As an intermediate pattern, "beans" or "varicose-vein" parallel stripes (Figure 5) evolve from the regular stripes and finally they split into blobs organized in a perfect rhombic array.

Any stable pattern obtained by sidewall forcing is stable after switching off the forcing ( $A_p = 0$ ), as well as to slight perturbations on the forcing parameters,  $\omega$  and  $A_p$ .

#### 4. Discussion

Rhombic arrays can be obtained by stretching the natural selected pattern, hexagons, along one of its symmetry axes. This phenomenon was recently explained by the Austin group [33] by applying the transformation

$$S: (x,y) \longrightarrow ((1+\bar{\beta})^{-1}x,y) \quad (7)$$

to a hexagonal pattern ( $\bar{\beta}$  small and positive). This transformation stretches the x-axis, which is one of the symmetry axes of the hexagonal array. It is possible to show that this transformation leads to the formation of rhombic arrays.

In our case, since the stretching due to sidewall forcing is not uniform along the x-axis, the transformation given by Eq.(7) is not valid here. For  $\omega = 0$ , the stretching is constant in time but it depends on the distance from the forcing ( $x=0$ ) namely, those points near the left boundary are stretched more than far from it. This stretching factor depends on the amplitude of forcing and on the ratio  $D_v/D_u$ . Any transformation to a hexagonal pattern of the form

$$S: (x,y) \longrightarrow (x^{p/q}/\mu, y) \quad (8)$$

represents the dependence of the stretching on the  $x$  position. In Eq.(8),  $p$  and  $q$  are integers,  $p > q$  and  $\mu$  is the stretching factor. Although, we have used  $x^{p/q}$  in Eq.(8), any function  $\phi(x) \in C^1[0,n]$ , with  $\phi'(x) > 0$  in  $(0,n)$  could be used instead.

Then, following [33], we deduce that the rhombic pattern  $U_R(\vec{r}, t)$  ( $\vec{r} = xi\vec{i} + yj\vec{j}$ ) can be described in the original hexagonal basis,  $\vec{k}_i$ , by

$$U_R(\vec{r}, t) = \sum_{i=1}^3 a_i \exp \left\{ i \vec{k}_i \cdot (S^{-1}\vec{r}) \right\} \quad (9)$$

and

$$\begin{aligned} \vec{k}_1 \cdot (S^{-1}\vec{r}) &= k_0 y \\ \vec{k}_2 \cdot (S^{-1}\vec{r}) &= k_0 \left\{ \frac{\sqrt{3}}{2} \vartheta(x) - \frac{y}{2} \right\} \\ \vec{k}_3 \cdot (S^{-1}\vec{r}) &= k_0 \left\{ -\frac{\sqrt{3}}{2} \vartheta(x) - \frac{y}{2} \right\} \end{aligned} \quad (10)$$

where  $\vartheta(x) = (\mu x)^{q/p}$  and  $a_i$  ( $i=1,2,3$ ) are the complex envelope functions of the hexagonal pattern, here spatially modulated by  $\vartheta(x)$ . Perfectly organized rhombic patterns, such as those shown in Figure 3b, are obtained for all array sizes of the array if  $\vartheta(x) \geq 1$ ,  $\forall x \in [1,n]$  (note that only two wave vectors are modified by this transformation). In the other case, competition between domains of hexagons and rhombi can be obtained (for  $\vartheta(x) = 1$ , for some  $x > 1$  and some  $\mu$ , the hexagonal basis is recovered).

For  $\omega > 0$ , Eq.(8) should be modified to account for the periodic modulation in time of the stretching factor.

On the other hand, the differences observed in the Turing scale between the value predicted by Eq.(4) and that calculated numerically for the rhombic array (Figure 4b) are not resolved by Eqs.(8-10). This distortion between the observed results and those expected for hexagons should be described by a more appropriate transformation. Calculations based on symmetry arguments to describe these phenomena will be published elsewhere.

Main resonant peaks occur for  $D_u = 3/n$ ,  $n=1,2,\dots$  at a critical wavenumber,  $k_c$ , given by

$$6 \left\{ k_c \pm \epsilon(\omega) \right\}^2 = n \quad n = 1,2,\dots \quad (11)$$

where  $\epsilon(\omega)$  accounts for the near resonant case; it is a decreasing function of  $\omega$ , such that  $\epsilon(\omega) = 0$  for the maximum allowable frequency of forcing. Substitution of  $k_c$  into Eq.(4) provides the allowable  $D_v$  for resonance.

Secondary resonant peaks (in amplitude) obeying the Farey sequence correspond to

$$12 \left\{ k_c \pm \epsilon(\omega) \right\}^2 = 2n + 1 \quad n = 1,2,\dots \quad (12)$$

Although, the values of  $D_u$  are proportional to the Farey elements, we did not find a correlation between the amplitude of the resonant peaks and the level of the Farey tree.

The height of the resonant peaks in Figure 3 increases with  $D_u$  as a consequence of the increase in the wavelength, i.e. less number of blobs for the same constant size of the array; 50 x 50. Renormalizing the size of the array with respect

to the observed wavelength leads to similar heights for the main resonant peaks but at a considerably higher computation costs.

In the temporal evolution to the rhombic array formation, "varicose-vein" stripes have been observed. Each one of the two interfaces of the stripes loses its stability to sinusoidal perturbations which are  $\pi$  out of phase, producing a set of "varicose-vein" parallel stripes [34] as a consequence of the periodic forcing.

The transition to the rhombic state near the resonant case when  $D_v$  is increased follows the following scheme: stripes  $\mapsto$  rhombi  $\mapsto$  multiple domains (usually characterized by a competition between hexagons and rhombi domains). For large values of  $D_v$ , the constant amplitude of the forcing (for the case of  $\omega = 0$ ) decays quicker to zero than when  $D_v$  is lower, since the range of the inhibitor increases too. Thus, the stretching factor  $\mu$  increases when  $D_v$  diminishes (for a constant value of  $D_u$ ). In this case, for high values of  $\mu$ , the system can no longer support blobs, thereby giving rise to the appearance of stripes. Small values of  $\mu$  (i.e. high values of  $D_v$ ) provide enough space between the blobs so that rhombi and defects can appear everywhere, thereby lead to a situation with multiple domains.

## 5. Conclusions

Perfect organization into a rhombic array has been obtained for the resonant case when laterally forcing a two-dimensional medium undergoing a Turing bifurcation. The nature of the observed phenomena is independent of the selected numerical model.

Periodic sidewall forcing has been found to strongly influence the selection of stationary pattern formation, namely; stripes, rhombic arrays and hexagonal lattices with "penta-hepta" defects have been obtained depending on the frequency of forcing. The familiar Farey sequence, usually observed in the temporal modulation of dynamical systems without spatial-terms, has been translated to a reaction-diffusion

system. This resonance is shown to re-organize the system into a perfectly ordered rhombic array. Symmetry considerations based on a non-uniform stretching along the x-axis have been used to describe this bifurcation.

Rhombic arrays have been observed experimentally [33] and numerically [35] in reaction-diffusion systems under spontaneous conditions for values of the control parameters close to those for hexagonal pattern formation (usually found with "penta-hepta" defects). Although the kind of bifurcation and symmetry reported here is different from those considered in the literature, we hope this paper will stimulate others to find new alternative ways for rhombic pattern formation and control of perfect formation of structures experimentally.

**Acknowledgements:** This work is supported in part by the "Xunta de Galicia" (Spain) under project number XUGA20611B93. Numerical calculations have been performed on the vectorial super computer Fujitsu VP2400 at "Centro de Supercomputación de Galicia, CESGA" (Spain). We want to thank to Dr. Alex L. Zheleznyak and E. Barillot for fruitful discussions and Prof. Carlos Pérez-García for a careful reading of this manuscript.

## REFERENCES

- [1] P. Coulet and D. Walgraef "Spatial forcing of 2D wave patterns". *Europhys. Lett.* 10 (1989) 525-531.
- [2] D. Walgraef "External forcing of spatio-temporal patterns". *Europhys. Lett.* 7 (1988) 485-491.
- [3] P. Coulet "Commensurate-incommensurate transition in nonequilibrium systems" *Phys. Rev. Lett.* 56 (1986) 724-727.
- [4] M. Lowe and M.P. Gollub "Solitons and the commensurate-incommensurate transition in a convecting nematic fluid" *Phys. Rev. A* 31 (1985) 3893-3897.
- [5] H.R. Brand "Phase dynamics with a material derivative due to a flow field". *Phys. Rev. A* 35 (1987) 4461-4463.
- [6] J.J. Niemela and R.J. Donnelly. "External modulation of Rayleigh-Bénard convection" *Phys. Rev. Lett.* 59 (1987) 2431-2434.
- [7] H. Riecke, J.D. Crawford and E. Knobloch. "Time-modulated oscillatory convection". *Phys. Rev. Lett.* 61 (1988) 1942-1945.
- [8] P.C. Hohenberg and J.B. Swift. "Hexagons and rolls in periodically modulated Rayleigh-Bénard convection". *Phys. Rev. A* 35 (1987) 3855.
- [9] M.C. Cross and P.C. Hohenberg. "Pattern formation outside of equilibrium". *Rev. Mod. Phys.* 65 (1993) 851-1112.
- [10] J.J. Taboada, A.P. Muñuzuri, V. Pérez-Muñuzuri, M. Gómez-Gesteira and V. Pérez-Villar. "Spiral breakup induced by an electric current in a Belousov-Zhabotinsky medium". Submitted to *Chaos* (1994).
- [11] A.P. Muñuzuri, M. Gómez-Gesteira, V. Pérez-Muñuzuri, V.I. Krinsky and V. Perez-Villar. "Parametric resonance of a vortex in an active medium". Submitted to *Phys. Rev. E* (1994).
- [12] A.P. Muñuzuri, V. Pérez-Muñuzuri, M. Gómez-Gesteira, V.I. Krinsky and V. Perez-

- Villar. "Mechanism of parametric resonance of vortices of excitable media". To appear in *Int. J. of Bif. and Chaos* 4(5) (1994).
- [13] A.S. Mikhailov. "Fundations of Synergetics I". Springer-Verlag (1990).
- [14] O. Steinbock, V. Zykov and S.C. Müller. "Control of spiral wave dynamics in active media by periodic modulation of excitability". *Nature* 366 (1993) 322-324.
- [15] J. Lauzeral, S. Metens and D. Walgraef. "On the phase dynamics of hexagonal patterns". *Europhys. Lett.* 24 (1993) 707-712.
- [16] L.M. Pismen. "Bifurcation of quasiperiodic and nonstationary patterns under external forcing" *Phys. Rev. Lett.* 59 (1987) 2740-2743.
- [17] S. Ciliberto, E. Pampaloni and C. Pérez-García. "Competition between different symmetries in convective patterns" *Phys. Rev. Lett.* 61 (1988) 1198-1201.
- [18] S. Ciliberto, P. Coulet, J. Lega, E. Pampaloni and C. Pérez-García. "Defects in roll-hexagon competition" *Phys. Rev. Lett.* 65 (1990) 2370-2373.
- [19] P. Cerisier, C. Pérez-García, C. Jamond and J. Pantaloni. "Wavelength selection in Bénard-Marangoni convection" *Phys. Rev. A* 35 (1987) 1949-1952.
- [20] E.L. Koschmeider. "Bénard cells and Taylor vortices". Cambridge Univ. Press. (1993).
- [21] M. Bestehorn. "Phase and amplitude instabilities for Bénard-Marangoni convection in fluid layers with large aspect ratio" *Phys. Rev. E* 48 (1993) 3622.
- [22] Q. Ouyang and H.L. Swinney. "Transitions from a uniform state of hexagonal and striped Turing patterns". *Nature* 352 (1991) 610-612.
- [23] P. De Kepper, J. Perraud, B. Rudovics and E. Dulos. "Experimental study of stationary Turing patterns and of their interaction with traveling waves in a chemical system". To appear in *Int. J. of Bif. and Chaos* 4(5) (1994).
- [24] V. Castets, E. Dulos, J. Boissonade and P. De Kepper. "Experimental evidence of a sustained Turing-type nonequilibrium chemical pattern". *Phys. Rev. Lett.* 64 (1990) 2953-2956.

- [25] B.A. Malomed, A.A. Nepomnyashchy and M.I. Tribelsky. "Domain boundaries in convection patterns". Phys. Rev. A 42 (1990) 7244-7263.
- [26] J. Millán-Rodríguez. "Influence of defects in the hexagon-roll transition in convective layers". To appear in Int. J. of Bif. and Chaos 4(5) (1994).
- [27] M.I. Rabinovich and L.S. Tsimring. "Dynamics of dislocations in hexagonal patterns". Phys. Rev. E 49 (1994) 35-38.
- [28] A.M. Turing "The chemical basis of morphogenesis". Phil. Trans. R. Soc. London. B237 (1952) 37-72.
- [29] J.D. Murray. "Mathematical Biology". Springer-Verlag, N.Y. (1989).
- [30] F. Baras and D. Walgraef. "Nonequilibrium chemical dynamics: From experiment to numerical simulations". Physica A 188 (1992) 1-468.
- [31] J. Nossek and T. Roska. Eds. "Cellular Neural Networks". IEEE Trans. on Circuits and Syst. I. 40 (March 1993).
- [32] A.P. Muñuzuri, V. Pérez-Muñuzuri, V. Pérez-Villar and L.O. Chua. "Spiral waves on a 2D array of nonlinear circuits". IEEE Trans. on Circuits and Syst. I. 40 (1993) 872-877.
- [33] Q. Ouyang, G.H. Gunaratne and H.L. Swinney. "Rhombic patterns: Broken hexagonal symmetry". Chaos 3 (1993) 707-711.
- [34] P. Hirshberg and E. Knobloch. "Zigzag and varicose instabilities of a localized stripe". Chaos 3 (1993) 713-721.
- [35] V. Dufiet and J. Boissonade. "Numerical studies of Turing patterns selection in a two-dimensional system". Physica A 188 (1992) 158-171.

## FIGURE CAPTIONS

**Figure 1:** Allowable values of  $D_v$  for Turing pattern formation as a function of the critical wavenumber,  $k_c$  in Eq.(4), for different values of  $D_u$ . Note that for a constant value of  $D_u$ ,  $k_c$  does not change quantitatively when increasing  $D_v$ .

**Figure 2:** Spontaneous formation of hexagonal arrays. Note the different orientations of the hexagon domains separated by "penta-hepta" defects. Some of the blobs are not completely split from their neighbors. Size of the array: 100 x 100 and time of calculation 20000 t.u.

**Figure 3:** Resonant peaks for three different values of  $D_u$ . For any value of the frequency of forcing,  $\omega$ , and  $D_v$  within the peaks, locking between the forcing and the Turing pattern was observed in the form of a perfectly organized rhombic array (no defects). The Farey sequence was observed for values of  $D_u = 1.2$  and  $2.0$ . For  $\omega = 0$ , the bifurcations between patterns is shown in Figure 4. For any  $\omega > 0$ , and values of  $\omega$  and  $D_v$  outside the resonant peaks, a disordered situation consisting of rhombi and hexagons was always observed.

The peaks amplitude has been normalized in all cases by  $\omega^{\max}/D_u$  ( $D_u = 1.0$ ,  $\omega^{\max} = 0.05$ ;  $D_u = 1.5$ ,  $\omega^{\max} = 0.70$ ;  $D_u = 3.0$ ,  $\omega^{\max} = 40.0$ ) in order to present the peaks with the same order of magnitude.

**Figure 4:** Parallel stripes (a),  $D_v = 36.4$ , rhombic array (b),  $D_v = 40.0$ , and domain of hexagons and rhombi (c),  $D_v = 43.0$ , for a continuous forcing in time and amplitude ( $\omega = 0$ ,  $A_p = 1$ ). The underneath figures (d)-(f) are their respective spatial Fourier transforms. For the stripes pattern (a), only one frequency is relevant, a pair of peaks in (d), while the Fourier transform of the rhombic state contains three pairs

of peaks, (e), and the magnitude of one pair is higher than the other two. The disordered situation shown in (c), corresponds in the Fourier space to a multitude of frequencies, (f). Note the perfect organization of the rhombic array where one of the wave vectors is perpendicular to the direction of forcing.

In all figures, blue color corresponds to the minimum value of the x-variable in Equation 6, while the red color corresponds to the maximum x-value. Size of the array: 50 x 50 and time of calculation: 50000 t.u. Left lateral sidewall forcing was used in all the cases.

**Figure 5:** Varicose-vein parallel stripes. This unstable behavior was observed for  $\omega = 0$  when the system evolves in time to a perfectly organized of rhombic array. Usually it was found for values of  $D_v$  close enough to the boundaries of the resonant peaks.

Colors and size of the array like in Figure 4. Time of calculation 16000 t.u. for the same parameters leading to Figure 4b.

**Table I:** Comparison of wavelengths obtained numerically,  $\lambda$ , with those predicted by Eq.(4),  $\lambda_{dis.}$ , and the continuous theory,  $\lambda_{cont.}$  [27]. Average values of the wavelengths were calculated for those patterns shown in Figure 4. In all cases, the prediction agrees with the observed results except for the rhombic array where a difference higher than 20% was found. Note also the differences (2%) between the wavelengths predicted by the continuous [27] and discrete theory (Eq.(4)).



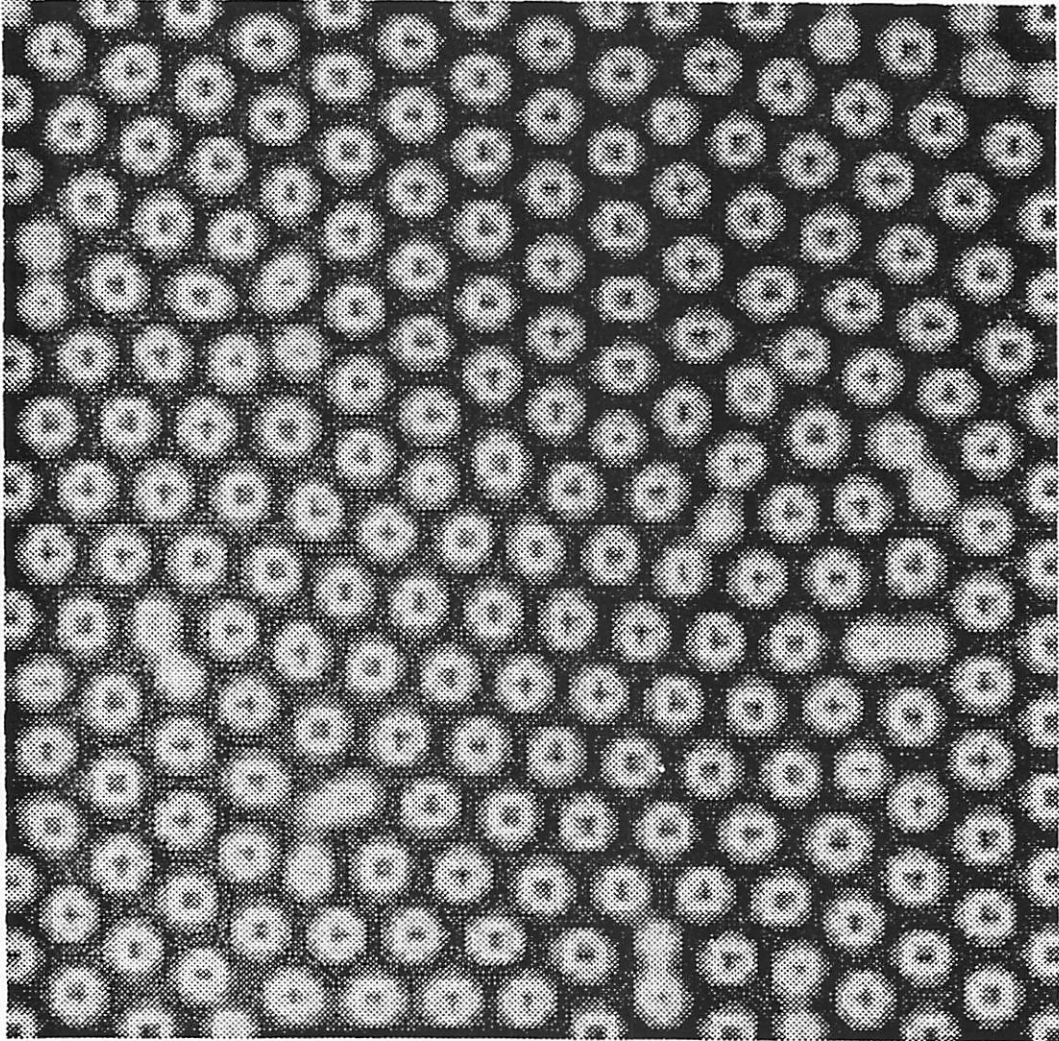


Figure c

v. Pireasthousian et al.

Color plate !!

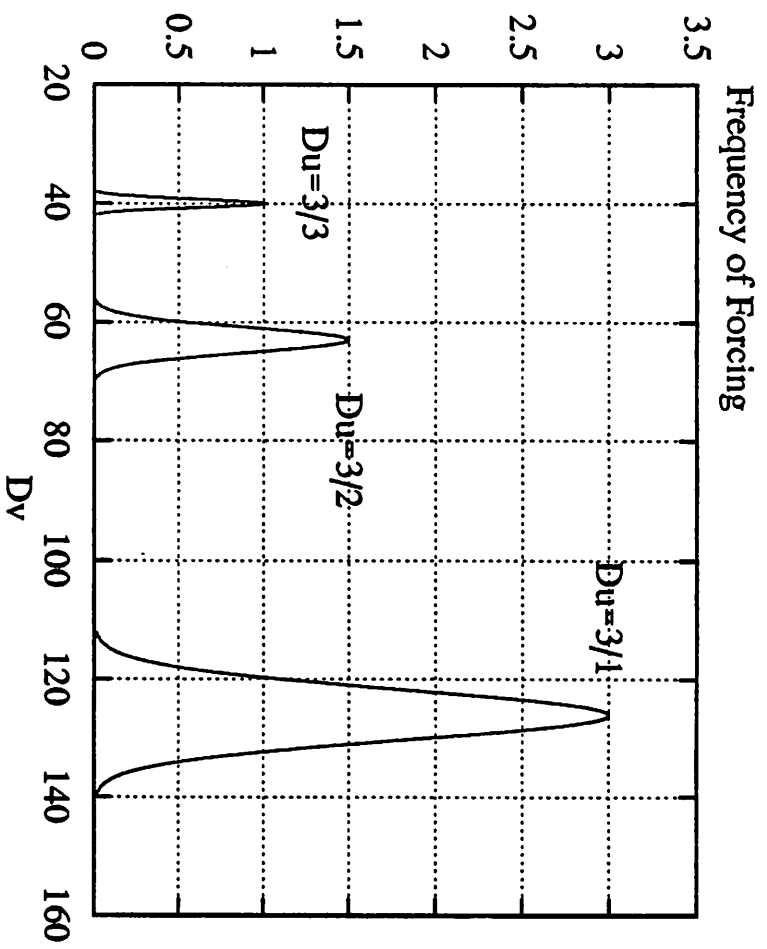


Figure 3

V. Pérez-Muñoz et al

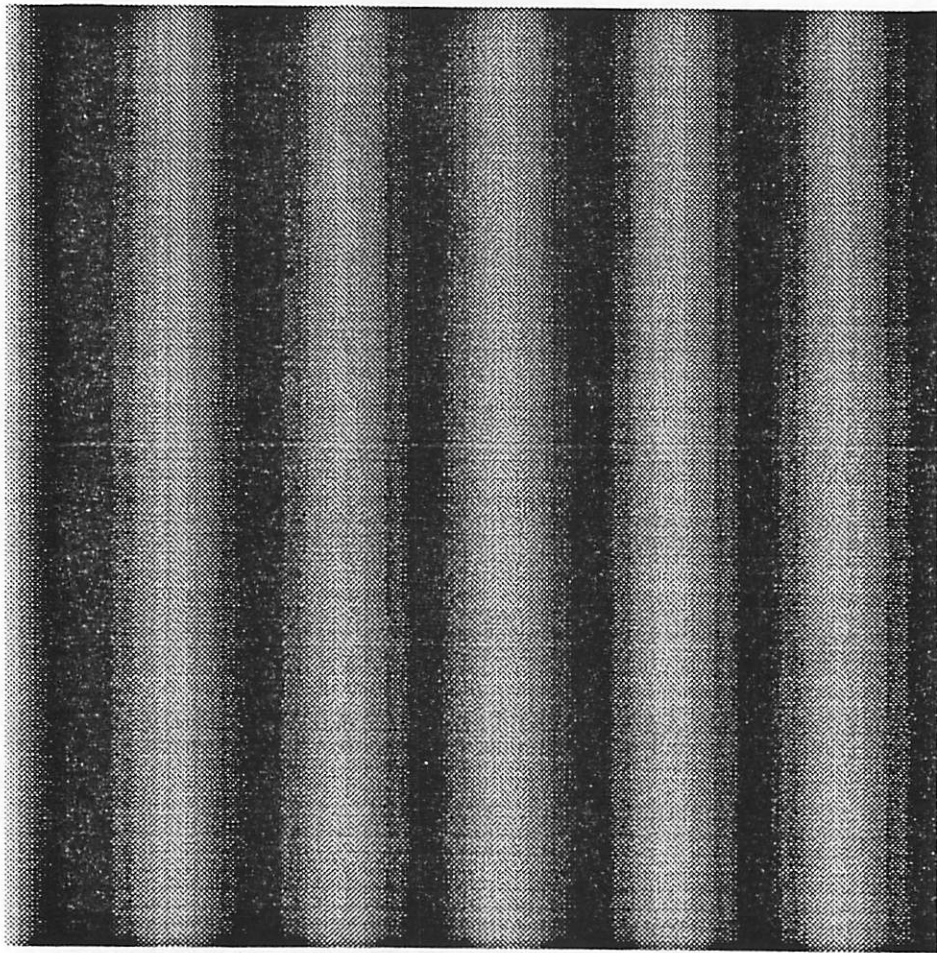


Figure 4a

V Pérez-Alvarez et al  
Cela plate !!

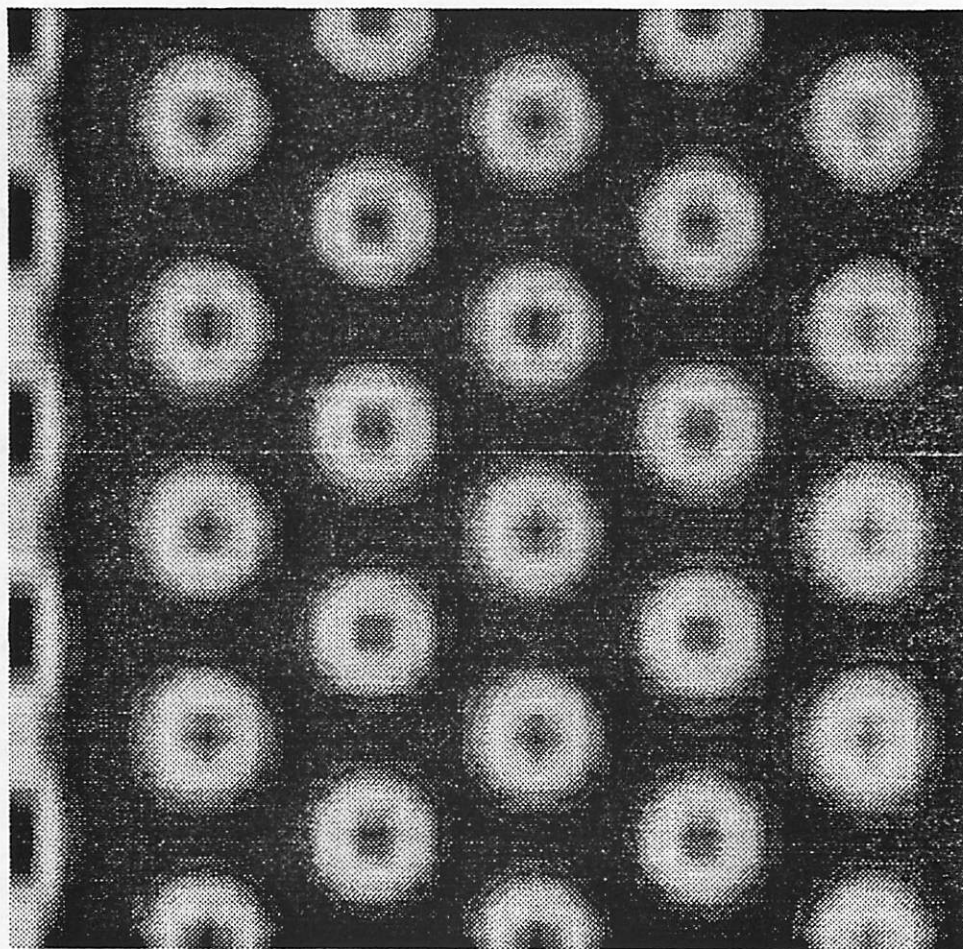


Figure 4b

V. Pérez-Minor et al.  
Color plate !!

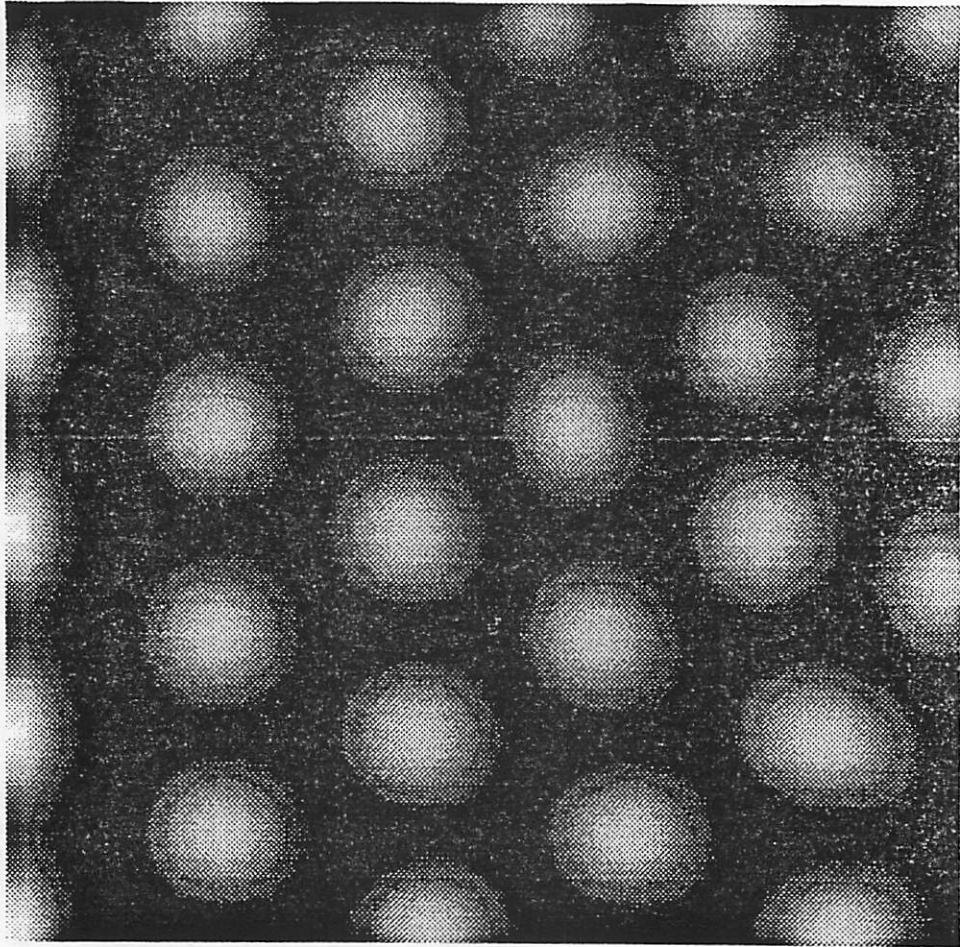


Figure 4c

V. Pérez - Miramón et al.

Colony plate !!

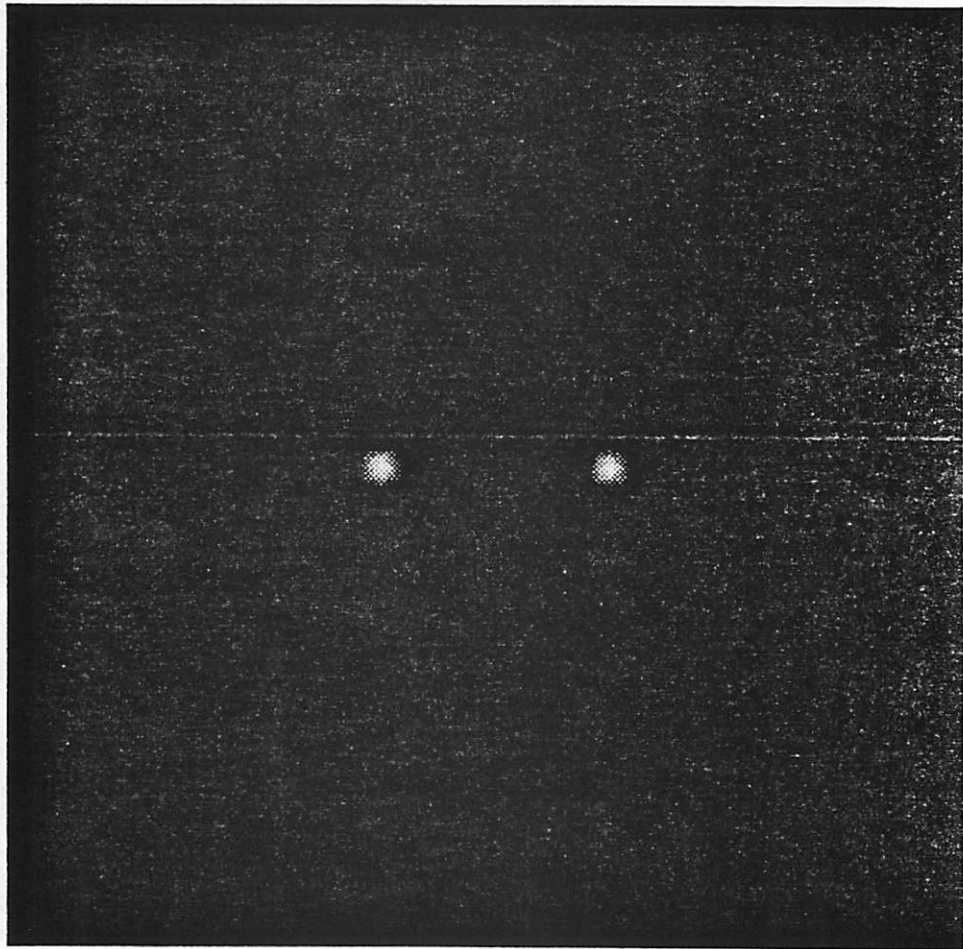


Figure 4d

V. Pérez-Muñoz et al  
Colloidal platelets

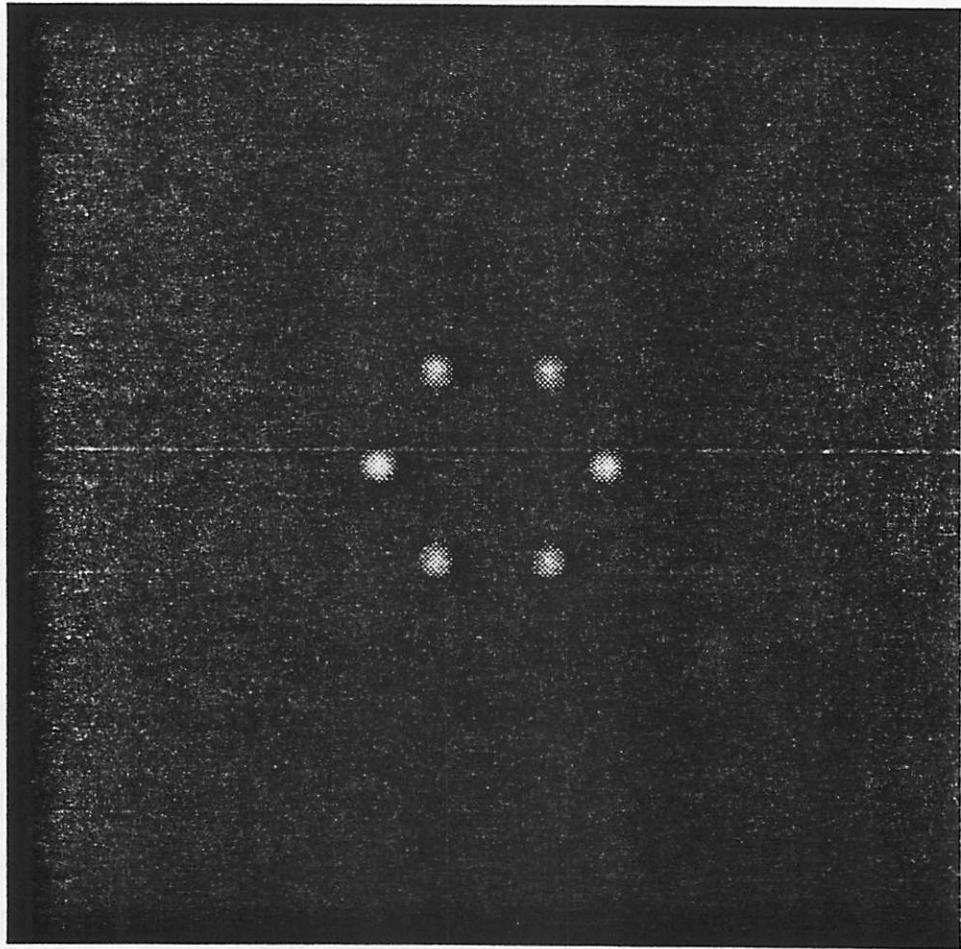


Figure 4c

V. Pérez-Muñoz et al

Cela, plate II

<b>Turing Pattern</b>	<b>Dv (Du = 1)</b>	$\lambda_{\text{dis.}}$ <b>Linear Stability</b>	$\lambda_{\text{cont.}}$ <b>Linear Stability</b>	$\lambda$ <b>Simulation</b>
<b>Parallel Stripes</b>	36.4	8.95	9.14	9
<b>Rhombic Array</b>	40.0	8.93	9.12	10.8
<b>Hexagons and Rhombi</b>	43.0	8.91	9.10	8.8

*Table I*